RESEARCH ARTICLE

Ralstonia solanacearum Uses Inorganic Nitrogen Metabolism for Virulence, ATP Production, and Detoxification in the Oxygen-Limited Host Xylem Environment

Beth L. Dalsing,[a,b] Alicia N. Truchon,[a] Enid T. Gonzalez-Orta,[a*] Annett S. Milling,[a*] Caitilyn Allen[a]

Department of Plant Pathology, University of Wisconsin—Madison, Madison, Wisconsin, USA[a]; Microbiology Doctoral Training Program, University of Wisconsin—Madison, Madison, Wisconsin, USA[b]

* Present address: Enid T. Gonzalez-Orta, Sacramento State University, Sacramento, California, USA; Annett S. Milling, R. J. Reynolds, Inc., Winston-Salem, North Carolina, USA.

ABSTRACT **Genomic data predict that, in addition to oxygen, the bacterial plant pathogen *Ralstonia solanacearum* can use nitrate (NO_3^-), nitrite (NO_2^-), nitric oxide (NO), and nitrous oxide (N_2O) as terminal electron acceptors (TEAs). Genes encoding inorganic nitrogen reduction were highly expressed during tomato bacterial wilt disease, when the pathogen grows in xylem vessels. Direct measurements found that tomato xylem fluid was low in oxygen, especially in plants infected by *R. solanacearum*. Xylem fluid contained ~25 mM NO_3^-, corresponding to *R. solanacearum*'s optimal NO_3^- concentration for anaerobic growth *in vitro*. We tested the hypothesis that *R. solanacearum* uses inorganic nitrogen species to respire and grow during pathogenesis by making deletion mutants that each lacked a step in nitrate respiration (Δ*narG*), denitrification (Δ*aniA*, Δ*norB*, and Δ*nosZ*), or NO detoxification (Δ*hmpX*). The Δ*narG*, Δ*aniA*, and Δ*norB* mutants grew poorly on NO_3^- compared to the wild type, and they had reduced adenylate energy charge levels under anaerobiosis. While NarG-dependent NO_3^- respiration directly enhanced growth, AniA-dependent NO_2^- reduction did not. NO_2^- and NO inhibited growth in culture, and their removal depended on denitrification and NO detoxification. Thus, NO_3^- acts as a TEA, but the resulting NO_2^- and NO likely do not. None of the mutants grew as well as the wild type *in planta*, and strains lacking AniA (NO_2^- reductase) or HmpX (NO detoxification) had reduced virulence on tomato. Thus, *R. solanacearum* exploits host NO_3^- to respire, grow, and cause disease. Degradation of NO_2^- and NO is also important for successful infection and depends on denitrification and NO detoxification systems.**

IMPORTANCE **The plant-pathogenic bacterium *Ralstonia solanacearum* causes bacterial wilt, one of the world's most destructive crop diseases. This pathogen's explosive growth in plant vascular xylem is poorly understood. We used biochemical and genetic approaches to show that *R. solanacearum* rapidly depletes oxygen in host xylem but can then respire using host nitrate as a terminal electron acceptor. The microbe uses its denitrification pathway to detoxify the reactive nitrogen species nitrite (a product of nitrate respiration) and nitric oxide (a plant defense signal). Detoxification may play synergistic roles in bacterial wilt virulence by converting the host's chemical weapon into an energy source. Mutant bacterial strains lacking elements of the denitrification pathway could not grow as well as the wild type in tomato plants, and some mutants were also reduced in virulence. Our results show how a pathogen's metabolic activity can alter the host environment in ways that increase pathogen success.**

Received 9 December 2014 **Accepted** 4 February 2015 **Published** 17 March 2015

Citation Dalsing BL, Truchon AN, Gonzalez-Orta ET, Milling AS, Allen C. 2015. *Ralstonia solanacearum* uses inorganic nitrogen metabolism for virulence, ATP production, and detoxification in the oxygen-limited host xylem environment. mBio 6(2):e02471-14. doi:10.1128/mBio.02471-14.

Editor Steven E. Lindow, University of California, Berkeley

Address correspondence to Caitilyn Allen, cza@plantpath.wisc.edu.

Diverse bacteria are capable of respiratory nitrate reduction, the membrane-bound conversion of nitrate (NO_3^-) to nitrite (NO_2^-), and denitrification, the stepwise enzymatic reduction of NO_2^- to nitrogen gas (N_2) via nitric oxide (NO) and nitrous oxide (N_2O). NO_3^- reduction and denitrification enable respiration in hypoxic or anaerobic environments because nitrogen oxides can serve as terminal electron acceptors (TEAs) in place of oxygen (O_2) (1). Bacterial NO_3^- respiration and denitrification are major drivers of the global nitrogen (N) cycle, of nutrient losses from soils, and of climate change (2–4). Though it has been extensively investigated in mutualistic N-fixing bacteria, the role of inorganic N metabolism in the virulence of plant pathogens is largely unexplored (5, 6). This may be because energetic metabolism has been seen as biologically distinct from virulence. However, bacteria need energy to produce virulence factors and grow inside the host, which are both essential processes for pathogenesis (7–9). Studies of several animal-pathogenic bacteria reveal that the host environment induces microbial nitrate respiration and/or denitrification and that these bacterial inorganic N reductions affect virulence (10–12).

The soilborne plant-pathogenic bacterium Ralstonia solanacearum invades plants through their roots. It aggressively colonizes the xylem elements in its host's vascular system, blocking water transport so that infected plants wilt and die (13). The bacterium

thrives in plant xylem, quickly reaching densities upwards of 10^9 CFU/g of stem tissue (14). This rapid growth is puzzling, because xylem sap is relatively nutrient poor and, presumably, low in O_2 (13, 15). *R. solanacearum* carries genes encoding three types of terminal oxidases (cytochrome *bd* oxidase, cytochrome *c* cbb_3-type oxidase, and cytochrome *c* aa_3-type oxidase). We previously found that one of the cbb_3-type oxidases is required for normal microaerobic growth and contributes significantly to the virulence and multiplication of *R. solanacearum* during plant infection (16). While these observations indicate that the pathogen uses O_2 during growth in the host, it is likely that *R. solanacearum* often encounters anaerobic conditions in its soil, rhizosphere, and plant habitats.

A preliminary analysis found that tomato xylem sap does contain significant levels of NO_3^-, which is an excellent TEA. In terms of redox potential, it is nearly as suitable as O_2 (16, 17). Additionally, in response to pathogen infection, plants, like mammals, typically produce NO, another potential electron sink for denitrifying microbes (1, 18). NO can also limit microbial growth by damaging DNA, sequestering important metal cofactors, and inhibiting terminal oxidase function to arrest aerobic respiration (19–22). High NO levels in host tissue could possibly force a plant pathogen to either use a TEA other than O_2 or halt growth.

The genome of *R. solanacearum* strain GMI1000 appears to encode a complete denitrification pathway, which includes a respiratory NO_3^- reductase (NarG), a NO_2^- reductase (AniA), a NO reductase (NorB), and a N_2O reductase (NosZ). The genome also includes a gene for a predicted flavohemoglobin (HmpX) that can detoxify NO either aerobically, by converting it to NO_3^-, or anaerobically, by converting it to N_2O. NorB can also convert NO anaerobically to N_2O (5). A transcriptomic analysis of *R. solanacearum* gene expression early in bacterial wilt disease revealed that all of these genes were highly expressed during tomato pathogenesis (17).

Together, these observations suggested that this vascular pathogen may respire and generate energy using inorganic N species as TEAs in low-O_2 and/or NO-rich microenvironments of plant xylem vessels. To test this hypothesis, we constructed a set of five single-gene deletion mutants of *R. solanacearum* strain GMI1000 that lacked *narG*, *aniA*, *norB*, *nosZ*, or *hmpX*. We analyzed the ability of these mutants to respire on NO_3^-, tolerate NO, grow in plants, and cause bacterial wilt disease. We found that although the bacterium respired on NO_3^- in the presence of O_2, NO_3^- respiration contributed directly to growth only under low-oxygen or anaerobic conditions. NO_2^- did not support bacterial growth; indeed, NO_2^- inhibited growth in a dose-dependent fashion. Both HmpX and NorB detoxified NO under aerobic and microaerobic conditions, but only NorB could degrade NO under anaerobic conditions. During plant infection, *R. solanacearum* quickly consumed O_2 and actively reduced inorganic N. NO_3^- respiration, denitrification, and aerobic NO detoxification all contributed to *R. solanacearum*'s growth *in planta.*

RESULTS

***Ralstonia solanacearum* expresses its inorganic nitrogen metabolic pathways *in planta* during bacterial wilt disease.** A recent transcriptomic study (17) found that predicted genes for NO_3^- respiration and denitrification were highly induced in *R. solanacearum* during tomato plant infection (Fig. 1A; see Table S1 in the supplemental material). The gene encoding the major catalytic

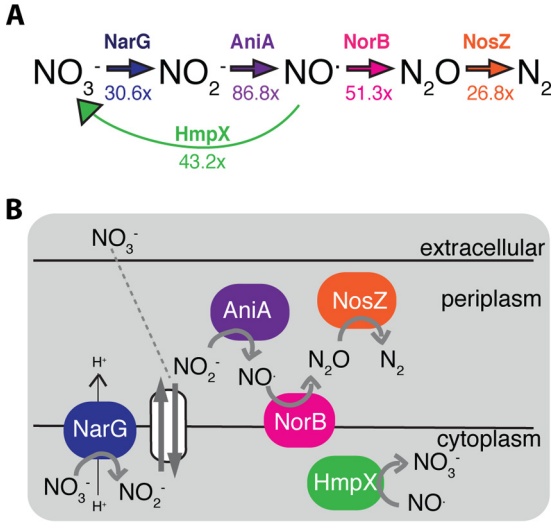

FIG 1 During tomato infection, *Ralstonia solanacearum* strain GMI1000 has high levels of expression of a complete nitrate respiration and denitrification pathway, including a nitric oxide detoxification system. (A) Inorganic N metabolic pathway with relevant enzyme shown above each reaction. The numbers below each reaction arrow indicate fold induction of the corresponding gene during plant infection relative to expression levels in culture (17). (B) Cellular context of NO_3^- respiration and denitrification. Following glycolysis and the citric acid cycle, electrons move through the electron transport chain to a terminal electron acceptor (TEA). In *R. solanacearum*, nitrate (NO_3^-), nitrite (NO_2^-), nitric oxide ($NO\cdot$), and nitrous oxide (N_2O) can potentially serve as TEAs. Data associated with each enzyme and its corresponding mutant are color coded consistently in all figures.

subunit of the predicted respiratory NO_3^- reductase (NarG) was expressed at 30.6-fold-higher levels *in planta* than in culture in rich CPG medium. CPG is composed of peptone, casamino acids, glucose, and yeast extract (with small amounts of NO_3^-) (23). Similarly, genes predicted to encode the catalytic subunits of NO_2^- reductase (AniA), NO reductase (NorB), and N_2O reductase (NosZ) were strongly induced *in planta* (86.8-fold, 51.3-fold, and 26.8-fold, respectively). In addition, the gene encoding the NO-detoxifying HmpX was also induced 43.2-fold during plant infection. The absolute expression values of these genes were among the highest in the bacterium's *in planta* transcriptome (see Table S1 in the supplemental material), indicating that *R. solanacearum* is actively metabolizing these inorganic N species during growth in host plant xylem vessels.

The general cellular context of the *R. solanacearum* denitrifying pathway and associated reactions, taken from genomic predictions, is shown in Fig. 1B (1). Briefly, NO_3^- can freely cross the outer cell membrane and is transported into the cytoplasm by NarK1 and/or NarK2 (24). In the cytoplasm, NarG reduces the NO_3^- to NO_2^-. This reaction pumps protons across the membrane into the periplasm, adding to the proton motive force generated in earlier steps of the electron transport chain. This proton motive force leads to ATP production. The NO_3^- importer exports NO_2^- from the cytoplasm to the periplasm, where AniA reduces it to NO. This reaction, along with the rest of the denitrification process, takes place in the periplasm and does not directly add to proton motive force. Instead, periplasmic reductase enzymes aid growth in some organisms by transferring electrons to their substrates, which allows for continued metabolic flow and continued proton motive force generation via early electron trans-

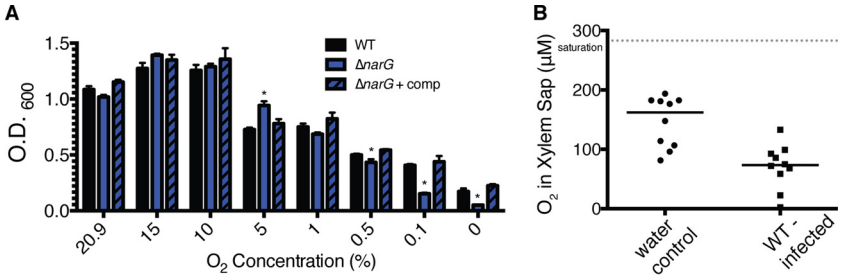

FIG 2 Nitrate respiration facilitates *Ralstonia solanacearum* growth at oxygen concentrations found *in planta*. (A) Culture densities (OD_{600}) of wild-type (WT), Δ*narG*, and complemented Δ*narG* strains of *R. solanacearum* following 24 h of incubation in VDM medium with 10 mM NO_3^- at a range of oxygen concentrations. The WT strain grew better at 15% and 10% O_2 than at 20.9% O_2 ($P = 0.0166$ and 0.0206, respectively). Each bar represents the mean result from 3 biological replicates, and error bars indicate standard errors of the means. *, significantly different from the result for the WT at the same O_2 concentration ($P < 0.05$, *t* test). (B) A Unisense multimeter microsensor was used to measure O_2 concentrations in xylem sap from wilt-susceptible tomato plants following soil soak inoculation with either water or wild-type *R. solanacearum*. Each point represents data collected from a single plant. Ten plants per treatment were sampled at the time of symptom onset. Horizontal bars indicate median values. The gray dotted line indicates O_2 saturation under these conditions. O_2 concentrations in sap from healthy and infected plants were different ($P = 0.0003$, *t* test).

port chain steps. In this way, NO is reduced by NorB. The resulting N_2O is reduced by NosZ to dinitrogen gas (N_2), which can freely dissipate into the extracellular environment.

To characterize the contributions of NO_3^- respiration, denitrification, and NO detoxification to *R. solanacearum*'s growth in culture, as well as to its growth and virulence in tomato plants, we generated five deletion mutant strains lacking the predicted *narG*, *aniA*, *norB*, *nosZ*, and *hmpX* genes, together with the corresponding complemented strains, with the exception of *nosZ* (see Table S2 in the supplemental material).

***R. solanacearum* uses *narG*-dependent nitrate respiration for growth under the low-oxygen conditions found *in planta* during disease.** Denitrification and NO_3^- respiration are typically low-O_2-to-anaerobic behaviors (1). To define the O_2 concentrations that support *R. solanacearum* NO_3^- respiration, we measured the growth of the bacterium supplied with NO_3^- in a range of atmospheric O_2 levels (20.9, 15, 10, 5, 1, 0.5, 0.1, and 0% O_2). To ensure maximum gas exchange, this growth assay was carried out in 10-ml cultures growing in 125-ml flasks. We used Van den Mooter (VDM) medium with 10 mM NO_3^-, which contains casamino acids, sodium succinate, magnesium sulfate, potassium phosphate, and KNO_3 and supports respiration of inorganic nitrogen by *R. solanacearum* (25). To determine how much NO_3^--supported growth was due to activity of the predicted NarG, we included the Δ*narG* mutant and its complemented strain in this assay. All of the strains tested grew best when supplied with 15 or 10% O_2 (Fig. 2A). However, *narG* was required for full growth at O_2 levels below 1%. The growth defect of the Δ*narG* strain was fully restored in the complemented Δ*narG* strain.

It has been postulated that bacteria experience a low-oxygen environment in plant xylem. To the best of our knowledge, however, the O_2 levels in infected tomato plants have not been directly measured (15). To determine whether the plant xylem is a permissive environment for bacterial NO_3^- respiration and denitrification, we used a microprobe to measure the O_2 content of tomato plant xylem sap. The xylem sap of healthy 3-week-old tomato plants contained 146.2 μM O_2 on average (Fig. 2B). There was no difference between O_2 measurements when the probe was inserted directly into xylem vessels or inserted into xylem sap accumulated on the surface of a newly cut stem (data not shown). We therefore took measurements from xylem sap accumulated on the cut stem surface, because this reduced the likelihood of breaking the delicate microprobe. Sap from healthy plants contained O_2 concentrations similar to those in sterile, nonaerated liquid growth medium (data not shown). However, xylem sap from plants infected with wild-type *R. solanacearum* contained significantly less oxygen, with an average of 70.87 μM O_2 ($P = 0.0003$, *t* test) (Fig. 2B). These values varied widely, ranging from 2.2 to 133 μM O_2. The lower O_2 concentrations were detected in plants with severe bacterial wilt symptoms, which harbored *R. solanacearum* populations of $>10^9$ CFU/g stem. The *in planta* data demonstrate that the bacterial wilt pathogen consumes O_2 in host tissue and therefore experiences a low-O_2 environment during plant infection, particularly at the later stages of disease. Although these *in planta* measurements are consistent with the *in vitro* findings described above, they cannot be directly compared. The probe measured molar concentrations of dissolved O_2, while the controlled-O_2 chamber used for the *in vitro* studies delivered a known percentage of atmospheric O_2.

Reduction of nitrate, nitrite, and nitric oxide is required for growth of *R. solanacearum* at wild-type rates under anaerobic conditions. We hypothesized that, in addition to NO_3^- respiration (Fig. 2A), the denitrification pathway of *R. solanacearum* is required for growth under anaerobic conditions in the presence of NO_3^-. We tested this by measuring the optical densities (ODs) of wild-type, Δ*narG*, Δ*aniA*, Δ*norB*, and Δ*nosZ R. solanacearum* strains following 24 h of stagnant anaerobic incubation in VDM medium with NO_3^- (Fig. 3A) (25). We included the Δ*hmpX* strain as a control because *hmpX* is not predicted to be involved in respiratory N metabolism but only in cytoplasmic NO consumption (26, 27). All of the strains tested reached endpoint optical densities below that of the wild-type parent strain, although the optical densities of the wild-type, Δ*nosZ*, and Δ*hmpX* strains were not significantly different. The Δ*narG*, Δ*aniA*, and Δ*norB* mutants grew less than the wild-type strain ($P < 0.05$, *t* test). The Δ*norB* strain had the most drastic growth defect. Adding a complementing wild-type gene fully or partially restored anaerobic growth on NO_3^- to all deletion mutants. The complemented Δ*aniA* strain did not reach wild-type levels, but this strain did grow significantly better than its Δ*aniA* parent ($P < 0.05$, *t* test). Under aerobic conditions, all strains grew equally well, and the results were statistically indistinguishable ($P > 0.05$, *t* test) (Fig. 3B).

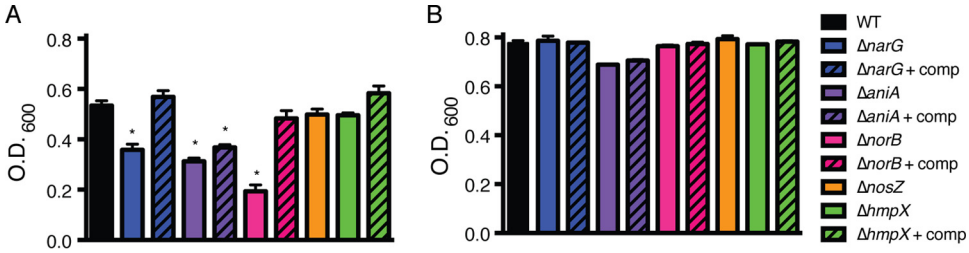

FIG 3 Nitrate, nitrite, and nitric oxide respiration contribute to *R. solanacearum*'s growth under anaerobic conditions. Growth of *R. solanacearum* strains was measured as the OD_{600} following 24 h of anaerobic (A) and aerobic (B) incubation in VDM medium with 10 mM NO_3^-. Bars show mean results for growth of 3 biological replicates, each containing 3 technical replicates. Error bars represent standard errors. *, significantly different from the result for the WT ($P < 0.05$, *t* test). Complementation did not fully restore the ability of all mutants to grow under these conditions, but each complemented strain grew better than its parent mutant ($P < 0.05$, *t* test).

Nitrate supports the growth of *R. solanacearum* in a dose-dependent manner, with an optimal concentration near that found *in planta*. To understand whether NO_3^- respiration and denitrification directly or indirectly contribute to bacterial growth, we tested the ability of wild-type *R. solanacearum* to grow under microaerobic (0.1% O_2) conditions in VDM medium with NO_3^- or NO_2^- concentrations ranging from 0 to 100 mM (Fig. 4A and 5A). While *R. solanacearum* grew no better on 10 μM or 100 μM NO_3^- than in the absence of NO_3^- (data not shown), the pathogen did grow better on NO_3^- at 1 mM ($P = 0.047$, repeated measures analysis of variance [ANOVA]), 10 mM ($P = 0.0098$, repeated measures ANOVA), 25 and 50 mM ($P = 0.0021$, repeated measures ANOVA), and 100 mM ($P = 0.0151$, repeated measures ANOVA). The bacterium grew optimally in culture at 25 to 50 mM NO_3^-. However, in 100 mM NO_3^-, the cultures had a much longer lag time, indicating that *R. solanacearum* is inhibited by high concentrations of either NO_3^- or its metabolic product, NO_2^-.

To connect these results to a relevant biological context, we measured NO_3^- in xylem sap from uninfected and *R. solanacearum*-infected tomato plants. Sap from both groups of plants contained 25 to 28 mM NO_3^- (Fig. 4B). This is similar to the NO_3^- concentration that best supported NO_3^--respiratory-dependent growth of *R. solanacearum* in culture.

In contrast, adding NO_2^- did not enhance low-O_2 growth of *R. solanacearum* at any level (Fig. 5A). In fact, cell growth was inhibited by 10 mM and 100 mM NO_2^-. This suggests that while NO_3^- respiration contributes directly to growth under oxygen limitation, denitrification only facilitates growth indirectly, by eliminating toxic levels of NO_2^- or by allowing the cell to release excess reducing power.

Nitrate is directly used as a terminal electron acceptor. Adenylate energy charge measures bacterial metabolic activity as indicated by the available energy momentarily stored in the adenylate system (28). To determine the contribution of NO_3^- respiration to *R. solanacearum*'s energy pool, we measured the levels of ATP, ADP, and AMP in cells of Δ*narG*, Δ*aniA*, Δ*norB*, Δ*nosZ*, Δ*hmpX*, and wild-type *R. solanacearum* growing under denitrification-conducive conditions in VDM medium plus NO_3^-. Wild-type *R. solanacearum* cells had a relatively high energy charge (~0.8), suggesting normal metabolic flow (28). At ~0.6, the Δ*narG* mutant had a significantly lower energy charge than its wild-type parent ($P = 0.0103$, *t* test) (Fig. 6). This suggests that the Δ*narG* strain is metabolically impaired, as would be expected if NO_3^- is used directly as a TEA. In *Escherichia coli*, an energy charge of 0.6 to 0.7 indicates inhibition of cell growth (28). The Δ*aniA* and Δ*norB* mutants had even lower average energy charges (~0.15 and ~0.09) than the Δ*narG* mutant ($P = 0.0021$

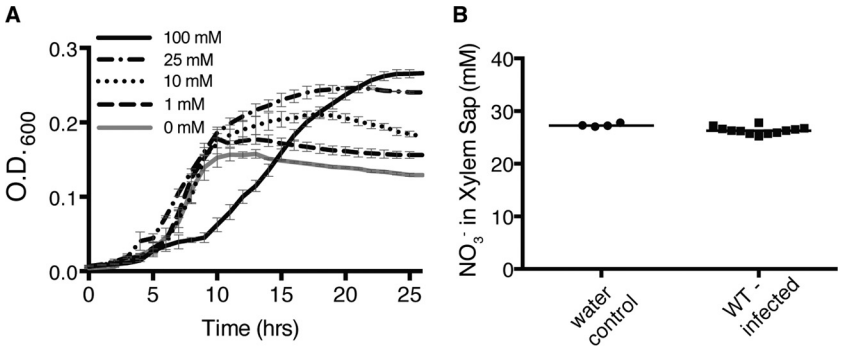

FIG 4 Nitrate directly supports the growth of *R. solanacearum* at biologically relevant concentrations. (A) Growth of wild-type *R. solanacearum* in 0.1% O_2 in VDM medium with various NO_3^- concentrations. Data are mean results from 3 biological replicates. Growth in 0 mM NO_3^- was significantly different from growth in 1 mM, 10 mM, 25 mM, 50 mM, and 100 mM NO_3^- ($P < 0.05$, repeated measures ANOVA). Growth in 50 mM NO_3^- (not shown) was indistinguishable from growth in 25 mM NO_3^-. Error bars represent standard errors. (B) Twenty-one-day-old wilt-susceptible tomato plants were inoculated with either water or wild-type *R. solanacearum*. At symptom onset, plant xylem sap was collected, and NO_3^- was quantified in each sample using Unisense multimeter NO_x and NO_2^- probes. Horizontal bars indicate mean values. Symbols indicate values from four plants inoculated with water and 12 plants inoculated with wild-type *R. solanacearum*.

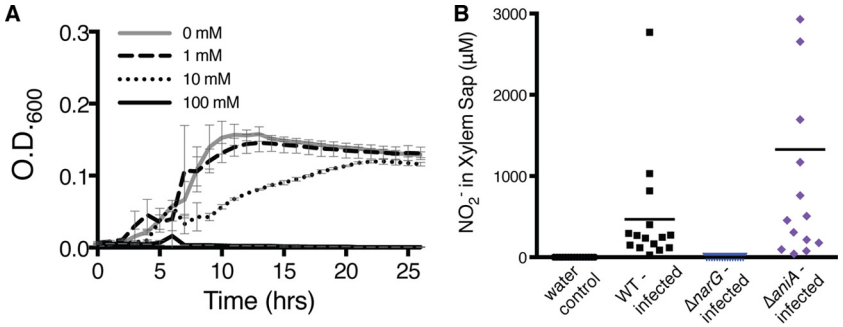

FIG 5 Nitrite inhibits *R. solanacearum*'s growth under low-oxygen conditions and is produced and consumed *in planta* via nitrate respiration and denitrification. (A) Growth of wild-type *R. solanacearum* in 0.1% O_2 in VDM medium with various NO_2^- concentrations. Data are mean results from 3 biological replicates. Growth with 0 mM NO_2^- was significantly different from growth with 10 mM and 100 mM NO_2^- ($P < 0.05$, repeated measures ANOVA). Error bars represent standard errors. (B) NO_2^- concentrations in xylem sap from tomato plants infected with wild-type (WT), Δ*narG*, or Δ*aniA R. solanacearum* or water-inoculated controls. At symptom onset, xylem sap was harvested and NO_2^- concentrations were determined using the Griess reaction. Horizontal bars indicate mean values, and each symbol represents the NO_2^- level in an individual plant. Xylem sap from plants infected with the Δ*aniA* mutant contained more NO_2^- than sap from plants infected with the WT ($P = 0.0337$, *t* test).

and 0.0007, respectively, *t* test). These data suggest that these two strains are metabolically blocked and may be accumulating toxic levels of NO_2^- and NO. In *E. coli*, a reading below 0.5 is incompatible with metabolic flow and eventually results in cell death (28). The energy charges of the Δ*nosZ* and Δ*hmpX* mutants (both ~0.75) were not different from that of the wild-type strain ($P = 0.0759$ and 0.1015, respectively, *t* test). These results, along with the finding that *narG* is essential for microaerobic or anaerobic growth and NO_2^- production, indicate that *R. solanacearum* uses NO_3^- as a TEA.

In culture, *R. solanacearum* produces and consumes nitrite under both aerobic and anaerobic conditions. To determine whether *R. solanacearum* performs NO_3^- respiration and denitrification under aerobic conditions, we quantified the NO_2^- produced by aerobic cultures in VDM medium supplied with NO_3^- (Table 1). Wild-type cells produced NO_2^- but Δ*narG* cells did not, indicating that NO_3^- reductase-mediated respiration is the source of the NO_2^- and that this reaction occurs when the bacterium grows aerobically. Cultures of the Δ*aniA* mutant accumulated more than twice as much NO_2^- as the wild type, consistent with the predicted NO_2^- reductase function of AniA. Interestingly, this result shows that NO_2^- respiration also occurs under aerobic conditions. However, inorganic N reduction did not contribute significantly to growth under aerobic conditions. We observed a similar pattern under anaerobic conditions (Table 1), although as expected, the cultures produced much more NO_2^- in the absence of O_2 and, as previously described (Fig. 3), this did contribute to growth. N_2 gas bubbles, which indicate complete denitrification, were present only when wild-type *R. solanacearum* grew anaerobically in liquid or semisolid medium containing NO_3^-. The Δ*narG*, Δ*aniA*, Δ*norB*, and Δ*nosZ* denitrification mutants did not produce gas bubbles under these conditions, but complementation restored gas production (data not shown).

Wild-type *R. solanacearum* cultures produced visible gas bubbles within 2 h after inoculation at high cell densities (2.5×10^8 CFU/ml) into VDM medium with 30 mM NO_3^-. This medium was used because it supports *R. solanacearum* NO_3^- respiration and complete denitrification, ending in the production of N_2 gas (25). Interestingly, NO_2^- production had not peaked at 2 HPI (hours postinoculation) but reached a maximum at 8 HPI (see Fig. S1 in the supplemental material).

***R. solanacearum* denitrifies and respires on nitrate during tomato infection.** To determine whether NO_3^- respiration and denitrification occur in the biologically relevant environment of a

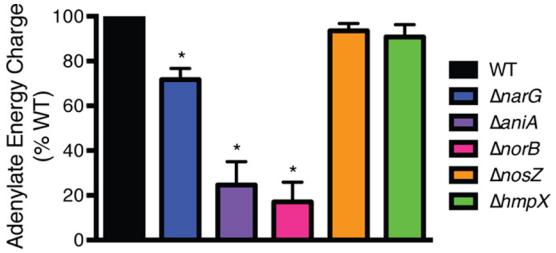

FIG 6 Relative energy charge levels indicate that *R. solanacearum* uses nitrate directly as a terminal electron acceptor. Cellular adenylate energy charge of wild-type and denitrification mutants incubated anaerobically in VDM medium with 10 mM NO_3^- for 20 h at 28°C was determined as described previously (28). Mean energy charges for each strain are shown as percentage of wild-type levels; data reflect 3 biological replicates, each with 3 technical replicates. Error bars show standard errors. *, significantly different from the WT result ($P < 0.01$, unpaired *t* test with Welch's correction).

TABLE 1 Nitrite and dinitrogen gas production under aerobic and anaerobic conditions

Genotype	NO_2^- production [μM (±SEM)] under indicated conditions[a]		N_2 production under anaerobic conditions[b]
	Aerobic	Anaerobic	
WT	43 (±8)	113 (±29)	+
Δ*narG*	0	0	−
Δ*aniA*	113 (±14)	9,066 (±976)	−

[a] NO_2^- concentrations were measured by Griess reaction after 20 h of growth under static anaerobic conditions or with shaking (225 rpm) under aerobic conditions in VDM medium with 10 mM NO_3^- at 28°C; the NO_2^- concentrations measured include any NO present. The starting OD_{600} for all strains was 0.08. Values in parentheses are standard errors of the means; the experiments included 3 biological replicates, each containing 3 technical replicates.

[b] N_2 was detected visually following static 28°C incubation of tubes containing liquid VDM medium with 10 mM NO_3^- inoculated with 10 μl of *R. solanacearum* strains at a range of cell densities. The same results were obtained when the assay was repeated in semisolid VDM medium with 10 mM NO_3^- and aerobic incubation at 28°C.

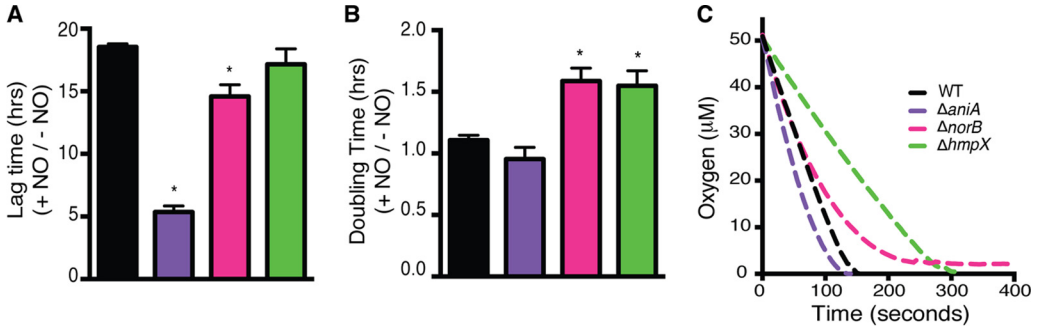

FIG 7 *R. solanacearum* detoxifies nitric oxide by denitrification under low-oxygen conditions and by HmpX under high-oxygen conditions. Overnight bacterial cultures in VDM medium without NO_3^- were pelleted, resuspended in fresh VDM medium without NO_3^-, and incubated for 4 h. Cultures were then diluted 1:10 in VDM medium with 10 mM NO_3^- and incubated statically for 2 h to induce the expression of denitrifying enzymes. One millimolar NO in the form of spermine NONOate was added to half of the wells, and the OD_{600} was read over 72 h. The growth of each strain with and without NO is shown as a ratio for lag time (A) and doubling time (B). *, significantly different from the WT result ($P < 0.05$, *t* test). The experiment was replicated 3 times with 3 technical replicates for each treatment; data from a representative assay are shown. Error bars indicate standard errors. (C) Oxidase inhibition assay. Overnight cultures were resuspended to uniform OD_{600} in fresh VDM medium with 10 mM NO_3^- and shaken aerobically for 3 h. One millimolar NO in the form of spermine NONOate was spiked into cultures, and O_2 consumption was tracked until concentrations reached 0 or plateaued. Data are means of results from 3 biological replicates.

host plant, we measured NO_2^- in xylem sap from tomato plants inoculated with wild-type *R. solanacearum*, the Δ*narG* mutant, the Δ*aniA* mutant, or water (Fig. 5B). Xylem sap from water control plants contained no detectable NO_2^-. Plants infected with wild-type *R. solanacearum* contained, on average, 466.6 μM NO_2^-. Xylem NO_2^- concentrations increased as pathogen populations in the stem increased and as disease severity increased. Sap from Δ*aniA* mutant-infected plants contained, on average, 1,327 μM NO_2^-, 2.8-fold more than plants infected by the wild type ($P = 0.0337$, *t* test). Sap from plants infected with the Δ*narG* mutant contained no detectable NO_2^-. These results demonstrate that *R. solanacearum* produces NO_2^- via NarG-driven NO_3^- respiration during infection and that plants are not a source of NO_2^- in their xylem fluid.

***R. solanacearum* uses a denitrification enzyme, NorB, and the flavohemoglobin HmpX to detoxify nitric oxide.** Our results suggested that some steps in denitrification could detoxify potentially harmful inorganic N species, so we characterized the responses of wild-type, Δ*aniA*, Δ*norB*, and Δ*hmpX R. solanacearum* strains to NO challenge. We challenged these NO metabolism-related *R. solanacearum* strains with NO and monitored recovery following NO exposure in a 96-well plate format with an automated plate reader in order to determine lag time and growth rate, measured as doubling time during log phase of each strain following exposure to NO. Strains lacking a gene involved in NO exposure recovery or detoxification would be expected to have a significantly prolonged lag time and, perhaps, a lowered growth rate or doubling time. Figure 7 shows the average growth doubling times (Fig. 7B) and lag times (Fig. 7A) of cultures treated with NO relative to those of untreated control cultures. Interestingly, NO had less effect on the culture lag times of the Δ*aniA* and Δ*norB* denitrification mutants than on the lag time of the wild-type strain. It is likely that endogenous accumulation of NO_2^- and NO in these mutants primed their remaining detoxification systems and, thus, decreased their response time to exogenous NO. However, exogenous NO had a greater effect on culture doubling time in the Δ*norB* and Δ*hmpX* strains than in the wild-type strain. This suggests that both denitrifying (NorB) and flavohemoglobin (HmpX) enzymes degrade exogenous NO.

NO can inhibit bacterial terminal oxidases (19). To determine whether the slowed growth of the Δ*norB* and Δ*hmpX* strains following NO exposure was due to oxidase inhibition, we directly measured O_2 consumption in cultures challenged with 1 mM NO (Fig. 7C) (19). Both mutant strains consumed O_2 significantly more slowly than wild-type *R. solanacearum*. Interestingly, the Δ*norB* mutant was unable to consume the last ~3 μM O_2, and although the Δ*hmpX* mutant consumed all of the O_2, it did so at a much lower rate. In contrast, the Δ*aniA* mutant consumed O_2 faster than the wild type. Together, these data suggest that NorB can detoxify NO under all O_2 conditions, while HmpX only degrades NO aerobically (down to ~3 μM O_2) but does so at a higher rate than NorB. This is in contrast to what was found in *Vibrio fischerii*, where Hmp functions under both aerobic and anaerobic conditions, while Nor functions only under anaerobic conditions (29). It seems likely that accumulating NO_2^- in cultures of the Δ*aniA* mutant activates NorB and/or HmpX. We speculate that NO_2^- binds NsrR, a predicted NO_2^--responsive transcriptional regulator with a putative binding site upstream from *norB*, thus activating the expression of *norB* (30). HmpX may also be under the transcriptional control of NsrR. The *R. solanacearum* genome encodes a putative NsrR, but its function has never been investigated in this species. Alternatively, NsrR may not influence the expression of *norB* and/or *hmpX* and these genes may instead be controlled by alternative NO_2^--responsive regulators. Posttranslational modifications, such as tyrosine nitration, may also play a role in the activation of NorB and/or HmpX function (31).

Nitrate respiration, denitrification, and nitric oxide detoxification all contribute to *R. solanacearum*'s growth *in planta*. The results described above suggest that *R. solanacearum* can use its NarG-AniA-NorB-NosZ-HmpX enzymes to respire on NO_3^-, denitrify NO_2^-, and detoxify NO. In addition, we demonstrated that in tomato xylem vessels, the bacterium encounters levels of O_2 and NO_3^- conducive to these processes. To determine whether metabolism of inorganic N species helps this pathogen colonize its host plants, we measured bacterial population sizes in tomato stems two and three days after inoculation through a cut leaf petiole. In addition to the growth of the wild-type strain, we also measured the growth of the Δ*narG*, Δ*aniA*, Δ*norB*, Δ*nosZ*, and Δ*hmpX* mutant strains and their corresponding complemented strains.

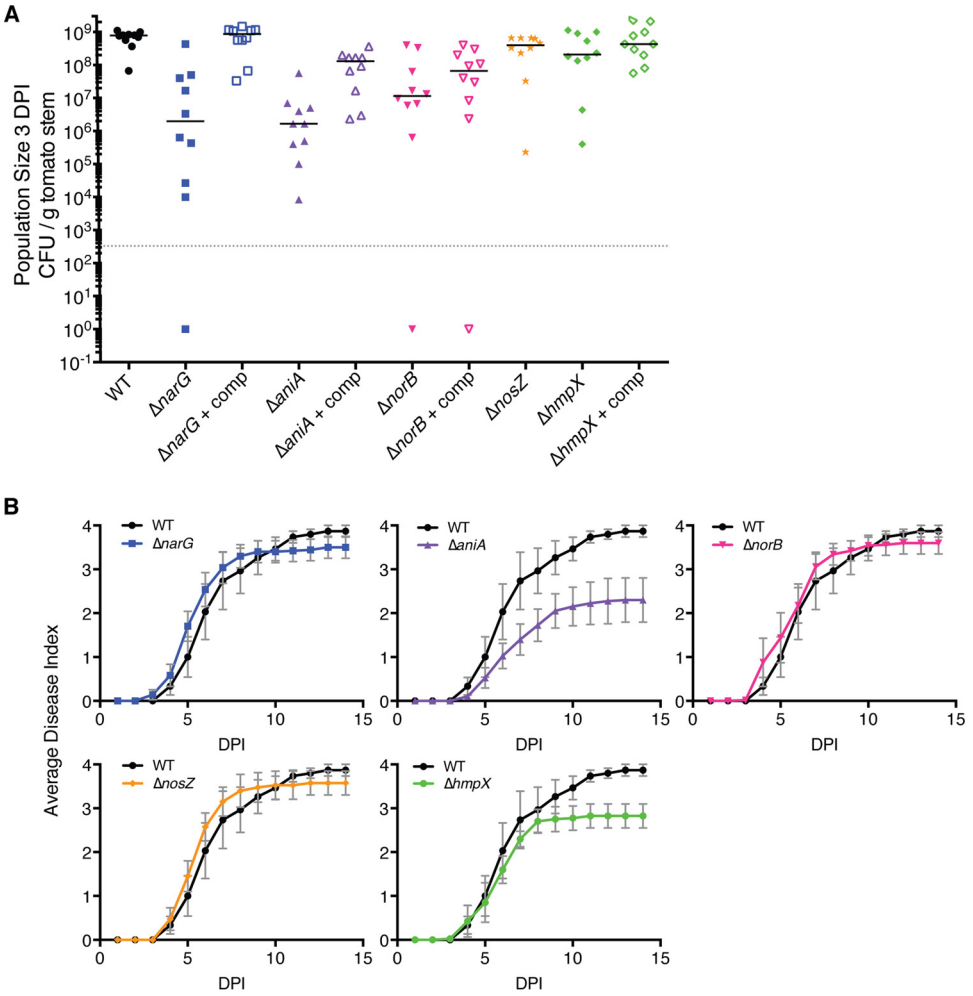

FIG 8 Respiratory nitrogen metabolism and nitric oxide degradation contribute to bacterial wilt virulence and support pathogen growth *in planta*. Twenty-one-day-old tomato plants were inoculated with 500 CFU of the specified *R. solanacearum* strains through a cut leaf petiole. (A) Bacterial growth *in planta*. At 3 days postinoculation (DPI), the pathogen population size in each plant was determined by grinding and dilution plating a 0.1-g stem section centered at the site of inoculation. Ten plants were sampled per strain; each symbol represents the bacterial population size in a single plant, and the horizontal bars indicate the median population size for each strain. The gray dotted line indicates the limit of detection; samples containing no detectable bacteria were given a value of 1. The wild-type strain grew significantly better *in planta* than all mutants tested; complementation restored growth of mutants, although not always to wild-type levels. Compared to the WT result, the *P* values for each strain's growth were as follows: Δ*narG*, $P < 0.0001$; Δ*narg* + comp (complemented Δ*narg* mutant), $P = 0.6371$; Δ*aniA*, $P < 0.0001$; Δ*ania* + comp, $P < 0.0001$; Δ*norB*, $P < 0.0001$; Δ*norb* + comp, $P < 0.0001$; Δ*nosZ*, $P = 0.0150$; Δ*hmpX*, $P = 0.0602$; and Δ*hmpx* + comp, $P = 0.411$. (B) Virulence assay. Plants were rated daily for 14 days using a disease index of 0 to 4. Data presented are mean results from 3 to 4 independent assays, each containing 10 plants per strain. Error bars indicate standard errors of the means. Disease progress curves of the Δ*aniA* and Δ*hmpX* mutants were significantly different from those of the WT strain ($P < 0.001$, repeated measures ANOVA).

All five mutant strains reached lower population sizes *in planta* than wild-type *R. solanacearum* at both 2 DPI (days postinoculation) (data not shown) and 3 DPI (Fig. 8A). At 3 DPI, the wild-type population sizes in the tomato plants differed from those of the Δ*narG*, Δ*aniA*, and Δ*norB* mutants ($P < 0.0001$, *t* test), as well as from that of the Δ*nosZ* mutant ($P = 0.0150$). The average population size of the Δ*hmpX* mutant was smaller than that of the wild type, but this difference was not significant ($P = 0.0602$). Adding the wild-type gene to the Δ*narG* mutant fully restored wild-type growth *in planta*. Complementing the Δ*aniA* and Δ*norB* mutants measurably restored growth *in planta*, though these strains still grew significantly less than the wild type. The poor *in planta* growth of mutant strains suggests that NO_3^- respiration, denitrification, and NO detoxification all contribute to host xylem colonization by *R. solanacearum*.

***R. solanacearum* needs nitrite reduction and nitric oxide detoxification for full virulence on tomato.** To assess the effects of inorganic N metabolism on bacterial wilt disease development, we measured the virulence of each mutant strain on tomato plants using the cut-petiole-inoculation assay described above. The Δ*aniA* and Δ*hmpX* mutants were significantly less virulent than the wild-type strain ($P < 0.0001$ and 0.0002, respectively, repeated measures ANOVA) (Fig. 8B). Although the Δ*narG*, Δ*norB*, and Δ*nosZ* mutants did not reach wild-type population sizes in tomato stems by 3 DPI, none of these mutants were reduced in virulence in this assay. Together, these data suggest that NO_3^- respiration, denitrification, and NO detoxification aid *R. solanacearum* in initial growth in the xylem but only NO_2^- reduction and NO detoxification are required for full virulence, at least when the bacteria are introduced directly into host xylem through a cut leaf petiole.

DISCUSSION

The goal of this study was to define the roles of inorganic N respiratory and detoxifying metabolism in *R. solanacearum*, especially during its pathogenic life inside plant host xylem. We recently showed that assimilation of NO_3^- contributes to *R. solanacearum*'s virulence and affects the production of extracellular polysaccharide, a virulence factor (32). We previously observed that a Tat secretion-defective mutant of K60, which cannot secrete its NO_3^- transporter or respire on NO_3^-, had reduced virulence on tomato, but this suggestive result did not prove that NO_3^- respiration itself contributes to bacterial wilt pathogenesis, as the Tat mutant was also defective in the secretion of other proteins unrelated to N metabolism (33). Little was known about NO_3^- reduction in this bacterium, possibly because Bergey's Manual describes the species *R. solanacearum* as incapable of denitrification (34). However, comparative genomic analysis revealed that *R. solanacearum* strains in phylotypes I (Asia) and III (Africa) have complete denitrification pathways. Most strains in phylotypes II (Americas) and IV (Indonesia) have the three enzymes that allow them to reduce NO_3^- to N_2O, but they lack the NosZ nitrous oxide reductase and, thus, cannot reduce N_2O to dinitrogen gas (N_2), the final step in a complete denitrification pathway (35, 36). These genomic data are supported by phenotypic analyses showing that most *R. solanacearum* strains can denitrify (25). Bergey's mischaracterization apparently arose because they defined denitrification as the production of N_2 gas bubbles during anaerobic growth on NO_3^- and they studied the type strain, K60, which belongs to phylotype II. N_2 bubbles are only produced by the *nosZ*-carrying phylotype I and III strains.

Genes encoding NO_3^- respiration, NO detoxification, and denitrification were highly differentially expressed *in planta*, suggesting that these processes specifically adapt *R. solanacearum* to conditions in plant xylem tissue. We tested this hypothesis using a set of five defined deletion mutants that each lacked one of these strongly upregulated genes. Each mutant was characterized with respect to NO_3^- respiration, denitrification, and NO detoxification in culture; their phenotypes functionally confirmed the sequence-based gene annotations.

The Δ*narG* mutant could not respire on NO_3^- and had significantly lower adenylate energy charge levels than its wild-type parent, indicating that *R. solanacearum* reduces NO_3^- to generate proton motive force and produce ATP. Additionally, wild-type *R. solanacearum* grew on NO_3^- in a dose-dependent fashion. The bacterium did not grow on NO_2^-, suggesting that it cannot use this molecule as an energy-generating TEA. In contrast, another betaproteobacterium, *Neisseria meningitidis*, can grow directly on NO_2^- (37). We observed low levels of background growth in VDM medium independent of NO_3^- and NarG function, suggesting that *R. solanacearum* has NO_3^--independent ways to obtain energy under anaerobic conditions, possibly via amino acid fermentation or Stickland reactions (38). Various modifications in the composition of VDM medium did not eliminate this low-level growth. However, the background growth did not obscure the significant differences between mutant and wild-type strains under any of the conditions studied.

Because O_2 is typically the preferred TEA, microbes tend to resort to NO_3^- respiration and denitrification only under anaerobic conditions (1). *N. meningitidis*, however, can denitrify aerobically when reactive nitrogen species (RNS) intermediates accumulate (39). Likewise, *R. solanacearum* reduced NO_3^-, NO_2^-, and NO in culture under both aerobic and anaerobic conditions. However, the reduction of these inorganic N species only supported bacterial growth under low O_2 concentrations (<1%).

Though NO_3^-, NO_2^-, and NO reductases all functioned aerobically in *R. solanacearum*, the final step of denitrification, the reduction of N_2O to N_2 by NosZ, did not. This suggests that *R. solanacearum* NosZ only functions under complete anaerobiosis, as is true of *Paracoccus denitrificans* and *Pseudomonas stutzeri* (40, 41). Under anaerobic conditions, the growth of the Δ*nosZ R. solanacearum* strain was statistically indistinguishable from that of the wild type. Nonetheless, the Δ*nosZ* strain consistently reached lower optical densities than its wild-type parent. Though the ability to reduce N_2O did not contribute greatly to *R. solanacearum*'s anaerobic growth, this consistent trend suggests that it may make a slight contribution. This could be biologically important for infection prior to xylem colonization. We are investigating this possibility further.

R. solanacearum reached different maximum readings for OD at 600 nm (OD_{600}) in culture depending on the experimental conditions of the growth assays. To determine the optimal O_2 concentration for growth, 10-ml cultures were shaken in 125-ml flasks to ensure maximum gas exchange. To determine the relative effects of anaerobiosis on the growth of the denitrifying mutants, the culture OD_{600} was measured after 24 h in 15-ml conical tubes under stagnant conditions. Finally, to determine the effects of differing nitrate concentrations on *R. solanacearum*, bacteria were cultured in 200-μl volumes in 96-well plates at 0.1% O_2. Because of these differences in culture method, we compared growth trends and differences among strains, rather than the final OD_{600} endpoints.

Why do *R. solanacearum* NO_3^- respiration and denitrification pathways operate even in the presence of O_2? First, the pathogen must rapidly adapt to major changes in O_2 tension as it moves from soil to plant and between microhabitats within the plant. Before it colonizes xylem vessels, *R. solanacearum* forms microcolonies on root surfaces; such microcolonies formed by *Pseudomonas aeruginosa* are oxygen limited (42). *In planta* measurements showed that over the course of infection, *R. solanacearum* itself lowers the O_2 content in xylem fluid. Active inorganic N metabolism may allow uninterrupted bacterial growth during transitions from an aerobic to an anaerobic habitat. Such transitions can be deleterious; for example, the metabolism of *Dinoroseobacter shibae* comes to a halt while denitrification is activated during the switch from aerobic to anaerobic respiration (43). Second, *R. solanacearum* may use denitrification to dissipate excess reducing power, as multiple *Paracoccus* species do with periplasmic nitrate reductases (44).

Third, *R. solanacearum* could use the denitrification pathway to protect itself from the damaging RNS NO_2^- and NO. These can be produced by the bacterium itself and, possibly, additionally by plant defense systems. They threaten the bacterium whether O_2 is present or not. Although both NorB and HmpX could degrade NO in the presence of O_2, HmpX was more efficient than NorB. However, HmpX was ineffective at less than 3 μM O_2, like *Pseudomonas aeruginosa*'s flavohemoglobin, which functions only under aerobic conditions (45). In *Salmonella enterica* and *Vibrio fischerii*, Hmp is the main aerobic NO detoxification system (26, 29). *Moraxella catarrhalis*, which has no HmpX equivalent, relies on its NorB homolog for NO detoxification (46). *R. solanacearum* may

have other minor NO detoxification systems, which would be evident in a Δ*norB* Δ*hmpX* double mutant. For example, *R. solanacearum* GMI1000 expresses two potential cytochrome *bd* oxidases during disease (see Table S1 in the supplemental material); these can also act as NO detoxification systems and have been shown to contribute to virulence in *Shigella flexneri* (47, 48).

These explanations are not mutually exclusive, although our data directly support the detoxification hypothesis. In aerobic culture, exogenously supplied NO inhibited terminal oxidase function in the Δ*norB* and Δ*hmpX* mutants, but strains that had intact *norB* and *hmpX* were unaffected (data not shown). Furthermore, in anaerobic culture, the Δ*norB* strain had a low adenylate energy charge and grew very poorly on NO_3^-. This was presumably the result of toxic accumulation of endogenous NO, which could not be removed by HmpX under anaerobic conditions. When challenged with exogenous NO under low-O_2 conditions, the Δ*norB* strain had a longer doubling time than the wild type, confirming that this mutant is impaired in NO detoxification. Additionally, in both aerobic and anaerobic culture, the Δ*aniA* strain produced and accumulated NO_2^-, which inhibits *R. solanacearum* at concentrations above 1 mM. This led to an early decline in cell density, an overall lower growth endpoint, and a low adenylate energy charge. Taken together, the results of our experiments in culture suggest that inorganic N reduction and detoxification are needed to protect *R. solanacearum* from RNS toxicity under both anaerobic and aerobic conditions.

Genomic analyses suggest that *R. solanacearum* has a complex cascade of regulators that could modulate inorganic N metabolism, and several of these putative regulators are strongly expressed during wilt disease (17, 35). It appears that NO_2^- induces the expression of either *norB* or *hmpX*, because the Δ*aniA* strain, which accumulates NO_2^-, could detoxify NO and resist oxidase inhibition better than its wild-type parent. Our data support *in silico* predictions of transcriptional regulator binding sites that suggest *norB* expression could be controlled by NsrR, a NO_2^--responsive regulator (30). Additionally, we could not fully restore the Δ*aniA* mutant to wild-type growth with complementation constructs that included either the *aniA* gene plus its upstream regulatory region or the *aniA* gene plus the upstream regulatory region and two downstream putative signal peptide-encoding genes, RSp1501 and RSp1502. The upstream regulatory region may also modify *norB* gene expression, as *in silico* predictions suggest (30). The detrimental effects of a second copy of this regulatory region could explain this partial complementation. In a possibly analogous situation, complementation of the *aniA* homolog in *Pseudomonas aeruginosa* was reported to be "slightly toxic" (49). We also observed that NO_3^- respiration and denitrification occurred mainly during late log or early stationary phase, hinting that this function could be modulated by one of *R. solanacearum*'s two quorum-sensing systems, as is the case in *P. aeruginosa* (50, 51).

The concentrations of O_2, NO, and NO_2^- are key regulatory signals for other denitrifying bacteria (1, 30, 52). Following detailed gene expression analyses in culture, biosensing fluorescent reporter constructs could be developed to nondestructively measure the levels of these compounds experienced by *R. solanacearum* over the course of plant infection. We speculate that bacteria aggregated on xylem vessel walls experience higher NO and NO_2^- levels than planktonic bacteria in flowing xylem fluid. It would also be interesting to determine how inorganic N respiration and detoxification affect biofilm formation, maintenance, and dispersal, which are dependent on inorganic N metabolism in *P. aeruginosa* (53, 54).

After exploring the roles of NO_3^- respiration, denitrification, and NO detoxification in *R. solanacearum* cells growing in culture, we characterized these metabolic behaviors in the biologically relevant plant environment. Our experiments in culture showed that the bacterium can use these pathways to grow in high NO_3^- concentrations over a range of O_2 levels. These were similar to the NO_3^- and O_2 levels that we detected in xylem sap from healthy and diseased tomato plants. NO_2^-, the product of NarG-mediated NO_3^- reduction, was present in sap from infected plants but not in sap from healthy plants. Furthermore, the NO_2^- concentration in sap increased with pathogen cell density and was dependent on *narG* and *aniA* function. Similarly, during macrophage infection, *Mycobacterium tuberculosis* uses NarG to produce NO_2^-, which influences the expression of many genes (55). This offers genetic and biochemical evidence that *R. solanacearum* reduces NO_3^- and NO_2^- *in planta* and indirectly suggests that the pathogen produces NO during infection. Attempts to use a microprobe to directly measure NO in xylem sap were unsuccessful, likely because both plant and microbial cells rapidly degrade this molecule, which is also chemically unstable (21). Notably, both NO_2^- and NO can affect plant defense signaling (56, 57). We are currently investigating the effects of *R. solanacearum* inorganic N metabolism on plant defense responses.

Direct measurements in plants infected by wild-type and mutant strains showed that *R. solanacearum* modifies its habitat by lowering the average O_2 concentration in the xylem. This is likely the result of bacterial oxidative respiration, because during tomato infection, *R. solanacearum* had high expression levels of genes for several predicted oxidases, including high-affinity oxidases likely to be effective under hypoxic conditions (see Table S1 in the supplemental material). The O_2 levels that we measured in xylem sap probably overestimate the amount of O_2 available to the pathogen in microhabitats such as bacterial aggregates on xylem vessel walls. It has been hypothesized that during intestinal infection, *Escherichia coli*'s anaerobic metabolism fluctuates to efficiently scavenge O_2 (58). We propose that *R. solanacearum* similarly consumes any available O_2 in xylem vessels, thereby creating an environment that requires the pathogen to use alternate TEAs, such as NO_3^-, during pathogenesis. Alternatively, the two TEAs may be used simultaneously during infection.

In response to pathogens, plants produce NO, an early component of the defense signal transduction pathway (57). The results of our *in vitro* experiments indicate that NO can also directly inhibit *R. solanacearum* by interfering with terminal oxidase function and that the pathogen protects itself from NO by converting the toxic molecule into either N_2O (via NorB) or NO_3^- (via HmpX, if O_2 is present) (5). The plant pathogen *Dickeya dadantii* requires HmpX for full virulence on *Saintpaulia* plants (59). Because *D. dadantii* cannot produce NO via denitrification or any other known enzymatic pathway, it must use HmpX to detoxify plant-produced NO (60). Our results suggest that *R. solanacearum* produces NO in culture (via denitrification) and encounters NO during infection. Do plants produce NO in response to *R. solanacearum*, or is the NO presumably encountered by the bacterium during infection the result of bacterial metabolism? Additionally, does the pathogen experience inhibitory levels of NO during infection, and if so, has the pathogen adapted to make use

of it? As shown above, *R. solanacearum* can use NO_3^- as a TEA to generate energy, so HmpX may play two synergistic roles by converting the host's chemical weapon into an energy source. This may be of particular importance in NO_3^--limited environments, such as in N-limited plants growing in low-input agriculture or natural ecosystems.

These data are consistent with the theory that plant pathogens nutritionally modify their host environment during infection (17, 61). One current paradigm is that the pathogen tricks its host into producing specific metabolites for the microbe's benefit. For example, *Salmonella enterica* serotype Typhimurium can use as a TEA the compound tetrathionate, which is produced by the host following pathogen-triggered oxidative stress (62). Our results suggest that the host environment can also be shaped by the pathogen's own metabolic activity in ways that increase pathogen success. We are currently pursuing broader metabolomic studies to better understand how this organism alters its host environment.

None of the denitrification or detoxification mutants grew as well in tomato stems as the wild-type parent. These growth defects may be due to the mutants' inability to degrade toxic RNS (for Δ*aniA*, Δ*norB*, Δ*hmpX*, and possibly, Δ*nosZ* strains) and an inability to access sufficient TEAs (for the Δ*narG* strain). The partial redundancy of NorB and HmpX, which can both detoxify NO, may explain why the Δ*norB* mutant does not have a bigger *in planta* growth defect and also has no virulence defect. Only the Δ*aniA* and Δ*hmpX* mutants had virulence defects following petiole inoculation. Because direct inoculation of bacteria into a cut leaf petiole strongly favors the pathogen, mutants must be seriously compromised to exhibit a virulence defect in this assay (63, 64). Thus, although the virulence defects of the Δ*aniA* and Δ*hmpX* mutants were relatively small, they are likely to be biologically relevant. Further experiments are needed to determine whether denitrification and N detoxification contribute to other steps in *R. solanacearum* pathogenesis, such as chemotaxis, root attachment and entry, biofilm formation and dispersal, and exit from necrotic tissue, as well as persistence in both plants and soil environments.

Taken together, these results suggest that, in host xylem, *R. solanacearum* experiences a high-inorganic N environment that is at least partly of its own making. To succeed under these conditions, *R. solanacearum* has adapted its N metabolism to take advantage of the opportunities offered by this resource and solve the problems posed by the associated growth-inhibitory RNS.

MATERIALS AND METHODS

Bacterial strains and culture conditions. The *Ralstonia solanacearum* strains and plasmids used in these experiments are listed in Table S1 in the supplemental material. *E. coli* was grown in Luria-Bertani (LB) medium at 37°C, and *R. solanacearum* was cultured in CPG medium at 28°C (23) unless otherwise noted. Antibiotics were used as needed at the following concentrations: 15 μg/ml gentamicin, 25 μg/ml kanamycin, and 10 μg/ml tetracycline. A modified Van den Mooter (VDM) medium was used for low-oxygen and anaerobic growth (25). To decrease the complexity of this undefined medium, we used 0.5% (wt/vol) Casamino acids instead of yeast extract. VDM medium without NO_3^- was buffered to a pH of 6.2 with 10 mM morpholineethanesulfonic acid (MES) and supplemented with NO_3^- or NO_2^- as specified in the figure legends. Difco Laboratories (Detroit, MI), Sigma-Aldrich (St. Louis, MO), and Fisher Scientific (Hanover Park, IL) were our chemical suppliers.

Strain construction. Clean deletion mutants of *R. solanacearum* strain GMI1000 lacking the complete open reading frame (ORF) of *narG*, *aniA*, *norB*, *nosZ*, or *hmpX* were generated via homologous recombination using targeted deletion constructs produced with splicing by overhang extension PCR (SOE PCR) as described previously (32). The corresponding complemented strains were constructed using the *R. solanacearum* genomic tools of Monteiro et al. (65). Briefly, the region of interest, including the native promoter, was amplified and inserted into the pENTR/D-TOPO vector (Invitrogen, Carlsbad, CA). Using Gateway technology, the region was then transferred to pRCT, which does not replicate in *R. solanacearum* (65). The complementing pRCT was then moved into the corresponding mutant via natural transformation (66), and antibiotic resistance was used to select strains that had incorporated a single copy of the complementing genomic region into the selectively neutral *att*Tn*7* site. PCR was used to confirm incorporation of the desired DNA fragment.

Growth assays. To initially identify the oxygen levels at which nitrate respiration contributed to cellular multiplication, 9-ml amounts of liquid VDM medium containing 10 mM KNO_3 were inoculated with 1-ml amounts of overnight cultures of *R. solanacearum* strains adjusted to an OD_{600} of 0.1 (~1×10^8 CFU/ml). The initial OD_{600} of the cultures was thus 0.01. The endpoint OD was measured following 24 h of incubation in an oxygen-controlled chamber ($InVivo_2$ 400; Ruskinn) set to a specified O_2 concentration with N_2 gas and with shaking at 225 rpm. The experiment was replicated three times.

Dose-dependent growth of *R. solanacearum* strains in 96-well plates on NO_3^- was measured continuously by a BioTek HT plate reader for 25 h in the Ruskinn $InVivo_2$ 400 at 0.1% O_2. VDM broth supplemented with various concentrations of NO_3^- was inoculated with wild-type *R. solanacearum* GMI1000 to an initial OD_{600} of 0.01. Dose-dependent growth on NO_2^- was measured identically, with the exception that KNO_2 was used in place of KNO_3.

The endpoint growth of all deletion and complemented strains was assessed both under conditions of 0.1% O_2 with shaking (data not shown) and under anaerobic conditions (Fig. 3) in an anaerobic jar (GasPak anaerobic system; BD). Each strain was cultured overnight in 5 ml of VDM broth with no added NO_3^- and incubated at 28°C with shaking at 225 rpm. These cultures were centrifuged at 6,000 rpm for 10 min and resuspended in sterile water to an OD_{600} of 0.1. One-milliliter amounts of these inocula were pipetted into 9-ml amounts of VDM broth containing 10 mM NO_3^-, bringing the initial OD_{600} to 0.01. The tubes were lightly capped, to allow gas exchange, and incubated in an anaerobic jar for 22 h at 28°C. The OD_{600} was then measured to determine the ability of each strain to grow without O_2 under these denitrification-conducive conditions. The means and standard errors of data collected from five biological replicates (each including three technical replicates) are presented in Figure 3 for each strain.

Inorganic nitrogen and oxygen measurements. The Griess reaction (67) was used to quantify the amount of NO_2^- (and indirectly, NO) produced by *R. solanacearum* cells under denitrification-supportive conditions. Overnight cultures of the indicated strains were set up as described above. Ten-milliliter amounts of VDM medium with 10 mM NO_3^- in 15-ml sterile conical tubes were inoculated with a final OD_{600} of 0.08 (Table 1) or 0.25 (see Fig. S1 in the supplemental material) of resuspended and washed bacterial cultures. The tubes were incubated anaerobically, in BD GasPak anaerobic systems, or aerobically, as specified. At indicated time points, cells were lysed. Briefly, cells were incubated at 95°C for 10 min, moved to −20°C for 10 min, and centrifuged for 1 min to collect cellular debris. Three hundred-microliter amounts of supernatants were transferred to 15-ml conical tubes containing 2.6-ml deionized water. One hundred microliters of Griess reagent (Molecular Probes, Inc.) was added to each tube. The OD_{548} was measured after 30 min of incubation at room temperature. NO_2^- was quantified by using standard curves generated with known concentrations of NO_2^-. The data presented represent the mean results and standard errors of three biological replica-

tions, each with three technical replicates. N_2 production was qualitatively monitored. If denitrification went to completion, meaning that NosZ was reducing N_2O, N_2 gas bubbles could be seen in VDM medium with 10 mM NO_3^- when incubated at 28°C under stagnant conditions. Adding 0.25% noble agar to the VDM medium with 10 mM NO_3^- helped in dinitrogen visualization.

The Griess method was also used to chemically quantify NO_2^- (and, indirectly, NO) in infected and noninfected tomato plant xylem sap. Three-week-old tomato plants (bacterial wilt-susceptible cv. Bonny Best) were grown in 80 g of Sunshine Redi-earth professional plant growth mix (Sun Gro Horticulture, Agawarm, MA) and watered daily with Hoagland's fertilizer, a commonly used nitrate-containing fertilizer. These plants were soil soak inoculated with 50 ml of the indicated *R. solanacearum* strains suspended in water to an OD_{600} of 0.1, giving a final inoculum of ~5×10^7 CFU/g soil (63). When symptoms appeared, plant xylem sap was harvested (32). Xylem sap was centrifuged to remove plant and bacterial cells, and 300 μl of the supernatant was subjected to the Griess reaction to determine the NO_2^- concentration. The NO_2^- (and NO) level in sap from one water-inoculated control plant was determined for each inoculated plant. The data presented are individual plant data, and horizontal bars indicate median values.

We directly measured the concentrations of NO_3^- and O_2 in xylem sap from infected and noninfected tomato plants using a Unisense multimeter and the relevant Clark-type electrode probe (Unisense, Aarhus, Denmark). Plants were soil soak inoculated with *R. solanacearum* as described above. For NO_3^- measurements, the NO_x (which measures NO_3^- and NO_2^-) and NO_2^- probes were used as recommended by the manufacturer. To determine NO_3^- measurements, NO_2^- probe data were subtracted from NO_x data from each plant sample. Oxygen was measured using the OX-50 Unisense probe calibrated according to the manufacturer's instructions. To minimize gas diffusion introduced through harvesting, these probes were inserted into xylem sap immediately as it accumulated on the cut stem of decapitated plants. Symptomatic plants were used for inorganic N and O_2 quantification. For each wild-type *R. solanacearum* GMI1000-infected plant sampled, one water-inoculated control plant was also sampled. To validate probe function, 2 to 3 sets of probes were used for each assay.

Nitric oxide tolerance. To determine the contribution of denitrification to NO tolerance and detoxification, the NO_3^- respiration, denitrification, and predicted NO detoxification mutant strains were subjected to NO challenge and their growth recovery was monitored. Each strain was cultured overnight in VDM medium with no added NO_3^-, the OD_{600} was adjusted to 0.3 (log phase), and the cultures were incubated for 4 additional hours at 28°C with shaking at 225 rpm. Twenty microliters of each culture was transferred to a well of a 96-well plate containing 160 μl of VDM medium with 10 mM NO_3^-. The plates were incubated statically at room temperature for 2 h to develop low O_2 conditions and activate bacterial NO_3^- sensing. Then, wells were inoculated with either 20 μl of 0.01 M NaOH or 20 μl of 10 mM spermine NONOate (Cayman Chemical) in 0.01 M NaOH (10 mM spermine NONOate will release 20 mM NO with a half-life of 39 min at 37°C, pH 7.4; the rate of release is higher at lower pHs [we used 6.2] and lower at lower temperatures [we used 28°C]). The plates were immediately covered with breathable tape and placed in the BioTek HD plate reader. The OD_{600} was monitored for 65 h, and lag time and doubling time were calculated. The results are presented as the ratio of doubling time with NO challenge to doubling time with no NO and the ratio of lag time with NO challenge to lag time with no NO.

To measure the capacity of NO to inhibit *R. solanacearum* oxidase function, we spiked cultures with NO and measured O_2 consumption as previously described (19). Overnight cultures were pelleted at 6,000 rpm for 10 min and resuspended in VDM medium with 10 mM NO_3^- to an OD_{600} of 0.5 (~5×10^8 CFU/ml). Cultures were shaken for 3 h aerobically at 225 rpm. Immediately prior to O_2 quantification, a 1-ml aliquot was spiked with 500 μM spermine NONOate (=1 mM NO) and shaken vigorously to ensure O_2 saturation. An O_2 microprobe (Unisense, Aarhus, Denmark) was then inserted into the tube, and O_2 (uM) was measured until the signal stabilized or reached 0. The rate of consumption of the last 50 μM O_2 was measured.

ATP quantification and energy charge measurements. *R. solanacearum* strains were cultured overnight in rich CPG medium, pelleted by centrifugation, and resuspended in liquid VDM medium with 10 mM NO_3^- to an OD_{600} of 1.0 (~1×10^9 CFU/ml). Two-milliliter amounts of these cultures were pipetted into sterile 15-ml conical tubes and incubated for 18 to 20 h anaerobically in jars as described above. Following incubation, 100 μl of each culture was used for population size determination via the dilution plating technique. One milliliter of the remaining culture was lysed, and ATP/ADP/AMP were extracted with hot ethanol. ADP was enzymatically converted to ATP with pyruvate kinase, and AMP was converted to ATP with pyruvate kinase and adenylate kinase as described (28). Once converted, total AMP, ADP, and ATP were quantified with luciferase using the Promega ATP Enliten kit. All enzymes and adenylate standards were purchased through Sigma-Aldrich (St. Louis, MO). Data were collected with a Centro XS^3 LB 960 microplate luminometer (Berthold Technologies, Germany). Data represent the mean results of three biological replicates, each with three technical replicates and are presented as percentages of the wild-type energy charge, determined using the following formula: [(ATP) + 0.5(ADP)]/([ATP) + (ADP) + (AMP)].

***In planta* growth assays.** To determine the contribution of each deleted gene to *R. solanacearum*'s multiplication in host plant tissue, 21-day-old tomato plants were inoculated with 500 cells of the indicated bacterial strain via cut petiole as described above. Plants were grown and cared for as described above. Three days after inoculation, 0.1 g of plant tissue that included and surrounded the site of inoculation was harvested, ground, and subjected to dilution plating to determine the pathogen population size. Ten plants were sampled for each treatment.

Virulence assays. To determine the contribution of each deleted gene to the virulence of *R. solanacearum* on wilt-susceptible tomato plants, 3-week-old Bonny Best plants were infected with 500 cells of the indicated bacterial strains via cut petiole inoculations as described previously (17). Plants were grown and cared for as described above. Plants were rated daily for symptom development over 2 weeks using a scale of 0 to 4, as follows: 0, no leaves wilted; 1, 1 to 25% of leaves wilted; 2, 26 to 50% of leaves wilted; 3, 51 to 75% of leaves wilted; and 4, 76 to 100% of leaves wilted. This experiment was repeated four times with 10 plants per treatment in each replicate.

SUPPLEMENTAL MATERIAL

Supplemental material for this article may be found at http://mbio.asm.org/lookup/suppl/doi:10.1128/mBio.02471-14/-/DCSupplemental.

Figure S1, TIF file, 1.6 MB.
Table S1, DOCX file, 0.1 MB.
Table S2, DOCX file, 0.1 MB.

ACKNOWLEDGMENTS

This research was funded by National Science Foundation grant IOS 1258082, USDA-Hatch project WIS01502, and the University of Wisconsin-Madison College of Agricultural and Life Sciences. B.L.D. was supported by a National Science Foundation predoctoral fellowship.

We gratefully acknowledge Jonathan M. Jacobs, Edward G. Ruby, Michael G. Thomas, Daniel Amador-Noguez, and Paul Weimer for helpful discussions.

REFERENCES

1. **Zumft WG.** 1997. Cell biology and molecular basis of denitrification. Microbiol Mol Biol Rev **61:**533–616.
2. **Cornwell JC, Kemp WM, Kana TM.** 1999. Denitrification in coastal ecosystems: methods, environmental controls, and ecosystem level controls, a review. Aquat Ecol **33:**41–54. http://dx.doi.org/10.1023/A:1009921414151.
3. **Kirchman DL.** 2012. Processes in microbial ecology. Oxford University Press, Oxford, United Kingdom.

4. **Conrad R**. 1996. Soil microorganisms as controllers of atmospheric trace gases (H2, CO, CH4, OCS, N2O, and NO). Microbiol Rev **60:**609–640.
5. **Poole RK**. 2005. Nitric oxide and nitrosative stress tolerance in bacteria. Biochem Soc Trans **33:**176–180. http://dx.doi.org/10.1042/BST0330176.
6. **Lucinski R, Polcyn W, Ratajczak L**. 2002. Nitrate reduction and nitrogen fixation in symbiotic association rhizobium-legumes. Acta Biochim Pol **49:**537–546.
7. **Cole JA**. 2012. Legless pathogens: how bacterial physiology provides the key to understanding pathogenicity. Microbiology **158:**1402–1413. http://dx.doi.org/10.1099/mic.0.059048-0.
8. **Barbier T, Nicolas C, Letesson JJ**. 2011. Brucella adaptation and survival at the crossroad of metabolism and virulence. FEBS Lett **585:**2929–2934. http://dx.doi.org/10.1016/j.febslet.2011.08.011.
9. **Abu Kwaik Y, Bumann D**. 2013. Microbial quest for food in vivo: "nutritional virulence" as an emerging paradigm. Cell Microbiol **15:**882–890. http://dx.doi.org/10.1111/cmi.12138.
10. **Filiatrault MJ, Picardo KF, Ngai H, Passador L, Iglewski BH**. 2006. Identification of *Pseudomonas aeruginosa* genes involved in virulence and anaerobic growth. Infect Immun **74:**4237–4245. http://dx.doi.org/10.1128/IAI.02014-05.
11. **Jones SA, Chowdhury FZ, Fabich AJ, Anderson A, Schreiner DM, House AL, Autieri SM, Leatham MP, Lins JJ, Jorgensen M, Cohen PS, Conway T**. 2007. Respiration of *Escherichia coli* in the mouse intestine. Infect Immun **75:**4891–4899. http://dx.doi.org/10.1128/IAI.00484-07.
12. **Van Alst NE, Picardo KF, Iglewski BH, Haidaris CG**. 2007. Nitrate sensing and metabolism modulate motility, biofilm formation, and virulence in *Pseudomonas aeruginosa*. Infect Immun **75:**3780–3790. http://dx.doi.org/10.1128/IAI.00201-07.
13. **Peeters N, Guidot A, Vailleau F, Valls M**. 2013. *Ralstonia solanacearum*, a widespread bacterial plant pathogen in the post-genomic era. Mol Plant Pathol **14:**651–662. http://dx.doi.org/10.1111/mpp.12038.
14. **Schell MA**. 2000. Control of virulence and pathogenicity genes of *Ralstonia solanacearum* by an elaborate sensory network. Annu Rev Phytopathol **38:**263–292. http://dx.doi.org/10.1146/annurev.phyto.38.1.263.
15. **Pegg GF**. 1985. Life in a black hole—the micro-environment of the vascular pathogen. Trans Br Mycol Soc **85:**1–20. http://dx.doi.org/10.1016/S0007-1536(85)80151-0.
16. **Colburn-Clifford J, Allen C**. 2010. A *cbb*3-type cytochrome C oxidase contributes to *Ralstonia solanacearum* R3bv2 growth in microaerobic environments and to bacterial wilt disease development in tomato. Mol Plant Microbe Interact **23:**1042–1052. http://dx.doi.org/10.1094/MPMI-23-8-1042.
17. **Jacobs JM, Babujee L, Meng F, Milling A, Allen C**. 2012. The in *planta* transcriptome of *Ralstonia solanacearum*: conserved physiological and virulence strategies during bacterial wilt of tomato. mBio **3**(4):e00114-12. http://dx.doi.org/10.1128/mBio.00114-12.
18. **Romero-Puertas MC, Perazzolli M, Zago ED, Delledonne M**. 2004. Nitric oxide signalling functions in plant-pathogen interactions. Cell Microbiol **6:**795–803. http://dx.doi.org/10.1111/j.1462-5822.2004.00428.x.
19. **Husain M, Bourret TJ, McCollister BD, Jones-Carson J, Laughlin J, Vázquez-Torres A**. 2008. Nitric oxide evokes an adaptive response to oxidative stress by arresting respiration. J Biol Chem **283:**7682–7689. http://dx.doi.org/10.1074/jbc.M708845200.
20. **Stevanin TM, Ioannidis N, Mills CE, Kim SO, Hughes MN, Poole RK**. 2000. Flavohemoglobin Hmp affords inducible protection for *Escherichia coli* respiration, catalyzed by cytochromes bo' or bd, from nitric oxide. J Biol Chem **275:**35868–35875. http://dx.doi.org/10.1074/jbc.M002471200.
21. **Hughes MN**. 2008. Chemistry of nitric oxide and related species. Methods Enzymol **436:**3–19. http://dx.doi.org/10.1016/S0076-6879(08)36001-7.
22. **Hernández-Urzúa E, Mills CE, White GP, Contreras-Zentella ML, Escamilla E, Vasudevan SG, Membrillo-Hernández J, Poole RK**. 2003. Flavohemoglobin Hmp, but not its individual domains, confers protection from respiratory inhibition by nitric oxide in *Escherichia coli*. J Biol Chem **278:**34975–34982. http://dx.doi.org/10.1074/jbc.M303629200.
23. **Hendrick CA, Sequeira L**. 1984. Lipopolysaccharide-defective mutants of the wilt pathogen *Pseudomonas solanacearum*. Appl Environ Microbiol **48:**94–101.
24. **Sharma V, Noriega CE, Rowe JJ**. 2006. Involvement of NarK1 and NarK2 proteins in transport of nitrate and nitrite in the denitrifying bacterium *Pseudomonas aeruginosa* PAO1. Appl Environ Microbiol **72:**695–701. http://dx.doi.org/10.1128/AEM.72.1.695-701.2006.
25. **Hayward AC, El-Nashaar HM, Nvdegger U, De Lindo LD**. 1990. Variation in nitrate metabolism in biovars of *Pseudomonas solanacearum*. J Appl Bacteriol **69:**269–280. http://dx.doi.org/10.1111/j.1365-2672.1990.tb01518.x.
26. **Bang IS, Liu L, Vazquez-Torres A, Crouch ML, Stamler JS, Fang FC**. 2006. Maintenance of nitric oxide and redox homeostasis by the *Salmonella* flavohemoglobin hmp. J Biol Chem **281:**28039–28047. http://dx.doi.org/10.1074/jbc.M605174200.
27. **Forrester MT, Foster MW**. 2012. Protection from nitrosative stress: a central role for microbial flavohemoglobin. Free Radic Biol Med **52:**1620–1633. http://dx.doi.org/10.1016/j.freeradbiomed.2012.01.028.
28. **Chapman AG, Fall L, Atkinson DE**. 1971. Adenylate energy charge in *Escherichia coli* during growth and starvation. J Bacteriol **108:**1072–1086.
29. **Wang Y, Dunn AK, Wilneff J, McFall-Ngai MJ, Spiro S, Ruby EG**. 2010. *Vibrio fischeri* flavohaemoglobin protects against nitric oxide during initiation of the squid-*Vibrio* symbiosis. Mol Microbiol **78:**903–915. http://dx.doi.org/10.1111/j.1365-2958.2010.07376.x.
30. **Rodionov DA, Dubchak IL, Arkin AP, Alm EJ, Gelfand MS**. 2005. Dissimilatory metabolism of nitrogen oxides in bacteria: comparative reconstruction of transcriptional networks. PLoS Comput Biol **1:**415–431. http://dx.doi.org/10.1371/journal.pcbi.0010055.
31. **Arasimowicz-Jelonek M, Floryszak-Wieczorek J**. 2014. Nitric oxide: an effective weapon of the plant or the pathogen? Mol Plant Pathol **15:**406–416. http://dx.doi.org/10.1111/mpp.12095.
32. **Dalsing BL, Allen C**. 2014. Nitrate assimilation contributes to *Ralstonia solanacearum* root attachment, stem colonization, and virulence. J Bacteriol **196:**949–960. http://dx.doi.org/10.1128/JB.01378-13.
33. **González ET, Brown DG, Swanson JK, Allen C**. 2007. Using the *Ralstonia solanacearum* Tat secretome to identify bacterial wilt virulence factors. Appl Environ Microbiol **73:**3779–3786. http://dx.doi.org/10.1128/AEM.02999-06.
34. **Garrity G, Brenner DJ, Staley JT, Krieg NR, Boone DR, De Vos P, Goodfellow M, Rainey FA, Schleifer K-H**. 2005. Bergey's manual of systematic bacteriology, 2nd ed, vol 2, part C. Springer, New York, NY.
35. **Remenant B, Coupat-Goutaland B, Guidot A, Cellier G, Wicker E, Allen C, Fegan M, Pruvost O, Elbaz M, Calteau A, Salvignol G, Mornico D, Mangenot S, Barbe V, Médigue C, Prior P**. 2010. Genomes of three tomato pathogens within the *Ralstonia solanacearum* species complex reveal significant evolutionary divergence. BMC Genomics **11:**379. http://dx.doi.org/10.1186/1471-2164-11-379.
36. **Remenant B, de Cambiaire JC, Cellier G, Jacobs JM, Mangenot S, Barbe V, Lajus A, Vallenet D, Medigue C, Fegan M, Allen C, Prior P**. 2011. *Ralstonia syzygii*, the blood disease bacterium and some Asian *R. solanacearum* strains form a single genomic species despite divergent lifestyles. PLoS One **6:**e24356. http://dx.doi.org/10.1371/journal.pone.0024356.
37. **Rock JD, Moir JW**. 2005. Microaerobic denitrification in *Neisseria meningitidis*. Biochem Soc Trans **33:**134–136. http://dx.doi.org/10.1042/BST0330134.
38. **Nisman B**. 1954. The Stickland reaction. Bacteriol Rev **18:**16–42.
39. **Rock JD, Mahnane MR, Anjum MF, Shaw JG, Read RC, Moir JW**. 2005. The pathogen *Neisseria meningitidis* requires oxygen, but supplements growth by denitrification. Nitrite, nitric oxide and oxygen control respiratory flux at genetic and metabolic levels. Mol Microbiol **58:**800–809. http://dx.doi.org/10.1111/j.1365-2958.2005.04866.x.
40. **Bergaust L, van Spanning RJ, Frostegård A, Bakken LR**. 2012. Expression of nitrous oxide reductase in *Paracoccus denitrificans* is regulated by oxygen and nitric oxide through FnrP and NNR. Microbiology **158:**826–834. http://dx.doi.org/10.1099/mic.0.054148-0.
41. **Honisch U, Zumft WG**. 2003. Operon structure and regulation of the *nos* gene region of *Pseudomonas stutzeri*, encoding an ABC-type ATPase for maturation of nitrous oxide reductase. J Bacteriol **185:**1895–1902. http://dx.doi.org/10.1128/JB.185.6.1895-1902.2003.
42. **Wessel AK, Arshad TA, Fitzpatrick M, Connell JL, Bonnecaze RT, Shear JB, Whiteley M**. 2014. Oxygen limitation within a bacterial aggregate. mBio **5**(2):e00992. http://dx.doi.org/10.1128/mBio.00992-14.
43. **Laass S, Kleist S, Bill N, Drüppel K, Kossmehl S, Wöhlbrand L, Rabus R, Klein J, Rohde M, Bartsch A, Wittmann C, Schmidt-Hohagen K, Tielen P, Jahn D, Schomburg D**. 2014. Gene regulatory and metabolic adaptation processes of *Dinoroseobacter shibae* DFL12T during oxygen depletion. J Biol Chem **289:**13219–13231. http://dx.doi.org/10.1074/jbc.M113.545004.
44. **Richardson DJ**. 2000. Bacterial respiration: a flexible process for a changing environment. Microbiology **146:**551–571.
45. **Arai H, Hayashi M, Kuroi A, Ishii M, Igarashi Y**. 2005. Transcriptional

regulation of the flavohemoglobin gene for aerobic nitric oxide detoxification by the second nitric oxide-responsive regulator of *Pseudomonas aeruginosa*. J Bacteriol **187:**3960–3968. http://dx.doi.org/10.1128/JB.187.12.3960-3968.2005.

46. **Wang W, Kinkel T, Martens-Habbena W, Stahl DA, Fang FC, Hansen EJ.** 2011. The *Moraxella catarrhalis* nitric oxide reductase is essential for nitric oxide detoxification. J Bacteriol **193:**2804–2813. http://dx.doi.org/10.1128/JB.00139-11.
47. **Borisov VB, Gennis RB, Hemp J, Verkhovsky MI.** 2011. The cytochrome *bd* respiratory oxygen reductases. Biochim Biophys Acta **1807:**1398–1413. http://dx.doi.org/10.1016/j.bbabio.2011.06.016.
48. **Giuffrè A, Borisov VB, Mastronicola D, Sarti P, Forte E.** 2012. Cytochrome *bd* oxidase and nitric oxide: from reaction mechanisms to bacterial physiology. FEBS Lett **586:**622–629. http://dx.doi.org/10.1016/j.febslet.2011.07.035.
49. **Zennaro E, Ciabatti I, Cutruzzola F, D'Alessandro R, Silvestrini MC.** 1993. The nitrite reductase gene of *Pseudomonas aeruginosa*: effect of growth conditions on the expression and construction of a mutant by gene disruption. FEMS Microbiol Lett **109:**243–250. http://dx.doi.org/10.1111/j.1574-6968.1993.tb06175.x.
50. **Denny TP.** 2006. Plant pathogenic *Ralstonia* species, p 573243–644. In Gnanamanickam SS (ed), Plant-associated bacteria. Springer, Utrecht, the Netherlands.
51. **Hassett DJ, Cuppoletti J, Trapnell B, Lymar SV, Rowe JJ, Yoon SS, Hilliard GM, Parvatiyar K, Kamani MC, Wozniak DJ, Hwang SH, McDermott TR, Ochsner UA.** 2002. Anaerobic metabolism and quorum sensing by Pseudomonas aeruginosa biofilms in chronically infected cystic fibrosis airways: rethinking antibiotic treatment strategies and drug targets. Adv Drug Delivery Rev **54:**1425–1443. http://dx.doi.org/10.1016/S0169-409X(02)00152-7.
52. **Zumft WG.** 2002. Nitric oxide signaling and NO dependent transcriptional control in bacterial denitrification by members of the FNR-CRP regulator family. J Mol Microbiol Biotechnol **4:**277–286.
53. **Yoon MY, Lee KM, Park Y, Yoon SS.** 2011. Contribution of cell elongation to the biofilm formation of *Pseudomonas aeruginosa* during anaerobic respiration. PLoS One **6:**e16105. http://dx.doi.org/10.1371/journal.pone.0016105.
54. **Falsetta ML, McEwan AG, Jennings MP, Apicella MA.** 2010. Anaerobic metabolism occurs in the substratum of gonococcal biofilms and may be sustained in part by nitric oxide. Infect Immun **78:**2320–2328. http://dx.doi.org/10.1128/IAI.01312-09.
55. **Cunningham-Bussel A, Zhang T, Nathan CF.** 2013. Nitrite produced by Mycobacterium tuberculosis in human macrophages in physiologic oxygen impacts bacterial ATP consumption and gene expression. Proc Natl Acad Sci U S A **110:**E4256–E4265. http://dx.doi.org/10.1073/pnas.1316894110.
56. **Wang R, Xing X, Crawford N.** 2007. Nitrite acts as a transcriptome signal at micromolar concentrations in Arabidopsis roots. Plant Physiol **145:**1735–1745. http://dx.doi.org/10.1104/pp.107.108944.
57. **Bellin D, Asai S, Delledonne M, Yoshioka H.** 2013. Nitric oxide as a mediator for defense responses. Mol Plant Microbe Interact **26:**271–277. http://dx.doi.org/10.1094/MPMI-09-12-0214-CR.
58. **Jones SA, Gibson T, Maltby RC, Chowdhury FZ, Stewart V, Cohen PS, Conway T.** 2011. Anaerobic respiration of *Escherichia coli* in the mouse intestine. Infect Immun **79:**4218–4226. http://dx.doi.org/10.1128/IAI.05395-11.
59. **Favey S, Labesse G, Vouille V, Boccara M.** 1995. Flavohaemoglobin HmpX: a new pathogenicity determinant in *Erwinia chrysanthemi* strain 3937. Microbiology **141:**863–871. http://dx.doi.org/10.1099/13500872-141-4-863.
60. **Boccara M, Mills CE, Zeier J, Anzi C, Lamb C, Poole RK, Delledonne M.** 2005. Flavohaemoglobin HmpX from Erwinia chrysanthemi confers nitrosative stress tolerance and affects the plant hypersensitive reaction by intercepting nitric oxide produced by the host. Plant J **43:**226–237. http://dx.doi.org/10.1111/j.1365-313X.2005.02443.x.
61. **Chen LQ, Hou BH, Lalonde S, Takanaga H, Hartung ML, Qu XQ, Guo WJ, Kim JG, Underwood W, Chaudhuri B, Chermak D, Antony G, White FF, Somerville SC, Mudgett MB, Frommer WB.** 2010. Sugar transporters for intercellular exchange and nutrition of pathogens. Nature **468:**527–532. http://dx.doi.org/10.1038/nature09606.
62. **Winter SE, Thiennimitr P, Winter MG, Butler BP, Huseby DL, Crawford RW, Russell JM, Bevins CL, Adams LG, Tsolis RM, Roth JR, Bäumler AJ.** 2010. Gut inflammation provides a respiratory electron acceptor for *Salmonella*. Nature **467:**426–429. http://dx.doi.org/10.1038/nature09415.
63. **Tans-Kersten J, Huang H, Allen C.** 2001. *Ralstonia solanacearum* needs motility for invasive virulence on tomato. J Bacteriol **183:**3597–3605. http://dx.doi.org/10.1128/JB.183.12.3597-3605.2001.
64. **Flores-Cruz Z, Allen C.** 2011. Necessity of OxyR for the hydrogen peroxide stress response and full virulence in *Ralstonia solanacearum*. Appl Environ Microbiol **77:**6426–6432. http://dx.doi.org/10.1128/AEM.05813-11.
65. **Monteiro F, Solé M, van Dijk I, Valls M.** 2012. A chromosomal insertion toolbox for promoter probing, mutant complementation, and pathogenicity studies in Ralstonia solanacearum. Mol Plant Microbe Interact **25:**557–568. http://dx.doi.org/10.1094/MPMI-07-11-0201.
66. **Bertolla F, Van Gijsegem F, Nesme X, Simonet P.** 1997. Conditions for natural transformation of *Ralstonia solanacearum*. Appl Environ Microbiol **63:**4965–4968.
67. **Ignarro LJ, Buga GM, Wood KS, Byrns RE, Chaudhuri G.** 1987. Endothelium-derived relaxing factor produced and released from artery and vein is nitric oxide. Proc Natl Acad Sci U S A **84:**9265–9269. http://dx.doi.org/10.1073/pnas.84.24.9265.